

Effect of Chemical Reaction on MHD Boundary Layer Flow of Williamson Nanofluid Embedded In a Porous Medium in the Consideration of Viscous Dissipation and Newtonian Heating

M.Lavanya¹, Dr.M.Sreedhar Babu², G.Venkata Ramanaih³

^{1,3}Research scholar, Dept. of Applied Mathematics, Y.V.University, Kadapa Andhra Pradesh, India.

²Dept. of Applied Mathematics, Y.V.University, Kadapa Andhra Pradesh, India.

Abstract: The consideration of nanofluids has been paid a good attention on the free convection; the analysis focusing nanofluids in porous media are limited in literature. Thus, the use of nanofluids in porous media would be very much helpful in heat and mass transfer enhancement. In this paper, the influence of magnetohydrodynamic, thermal radiation, Newtonian heating and chemical reaction on heat and mass transfer over a horizontal linearly stretching sheet embedded in a porous medium filled with a nanofluid is discussed in detail. The solutions of the nonlinear equations governing the velocity, temperature and concentration profiles are solved numerically using Runge-Kutta Gill procedure together with shooting method and graphical results for the resulting parameters are displayed and discussed. The influence of the physical parameters on skin-friction coefficient, local Nusselt number and local Sherwood number are shown in a tabulated form.

Keywords: MHD, nanoparticle, Newtonian heating, porous medium, viscous dissipation, Williamson fluid model.

I. Introduction

Nanofluids are the fluid suspensions of nanoparticles showing many interesting properties and distinctive features. Al, Cu, Fe and Titanium or their oxides are the most frequently used nanoparticles. The materials with the sizes of nanometers possess unique physical and chemical properties. This led to the study of nanofluids in a variety of processes which resulted in notable applications in engineering and sciences. On account of its practical applications in industries, a great deal of attention is being paid to the research works on convective heat transfer in nanofluids in porous medium. [3] introduced the term nanofluids to denote to the fluid with incomplete nanoparticles. [2] confirmed that the adding of a small quantity of nanoparticles to conventional heat transfer liquids increases the thermal conductivity of the fluid up to in the region of two times.[1] discussed convective transport in nanofluids.He reported that only Brownian diffusion and thermophoresis are essential slip Mechanisms in nanofluids.

In many realistic cases, the heat transfer from the surface is relative to the local surface temperature. Such an effect is known as Newtonian heating effect. [9] investigated conjugate convective flow with Newtonian heating. Due to various applications researchers are attracted to consider the Newtonian heating condition within their problems. [6] presented an exact examination of mass and heat transfer past a vertical plate with Newtonian heating. Recently, the unsteady boundary layer flow and heat transfer of a Casson fluid under the Newtonian heating boundary condition for non-Newtonian fluid was studied by[7]. [4] concluded that the thermal radiation and Newtonian heating, both have raising effects on the fluid temperature and concentration decreases with increasing chemical reaction and Schmidt number.

However, consideration of nanofluids has been paid a good attention on the free convection; the analysis focusing nanofluids in porous media are limited in literature. Thus, the use of nanofluids in porous media would be very much helpful in heat and mass transfer enhancement. In this paper, the influence of magnetohydrodynamic, thermal radiation, Newtonian heating and chemical reaction on heat and mass transfer over a horizontal linearly stretching sheet embedded in a porous medium filled with a nanofluid is discussed in detail. The solutions of the nonlinear equations governing the velocity, temperature and concentration profiles are solved numerically using Runge-Kutta Gill procedure together with shooting method and graphical results for the resulting parameters are displayed and discussed. The influence of the physical parameters on skin-friction coefficient, local Nusselt number and local Sherwood number are shown in a tabulated form.

II. Mathematical Formulation

Consider a two-dimensional steady viscous flow of an electrically conducting viscous incompressible Williamson nanofluid through a stretching surface embedded with porous medium. The plate is stretched along x-axis with a velocity ax , where $a > 0$ is stretching coefficient. The fluid velocity, temperature and nanoparticle concentration near surface are taken to be U_w , T_w and C_w , respectively, which are as illustrated in figure A.

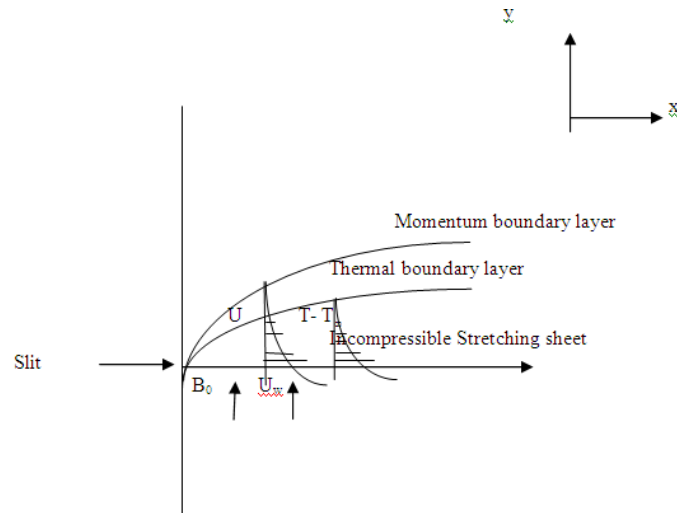


Fig. A: Schematic diagram of the boundary layer flow over Stretching sheet

With the usual Boussinesq and the boundary layer approximations, the governing equations of continuity, momentum, energy and volumetric species are written as follows

$$\frac{\partial u}{\partial x} + \frac{\partial v}{\partial y} = 0 \tag{2.1}$$

$$u \frac{\partial u}{\partial x} + v \frac{\partial u}{\partial y} = \nu \frac{\partial^2 u}{\partial y^2} + \sqrt{2\nu} \frac{\partial u}{\partial y} \frac{\partial^2 u}{\partial y^2} - \frac{\sigma B_0^2}{\rho} u - \frac{\nu}{k'} u \tag{2.2}$$

$$u \frac{\partial T}{\partial x} + v \frac{\partial T}{\partial y} = \alpha_f \frac{\partial^2 T}{\partial y^2} + \tau \left[D_B \frac{\partial C}{\partial y} \frac{\partial T}{\partial y} + \frac{D_T}{T_\infty} \left(\frac{\partial T}{\partial y} \right)^2 \right] - \frac{1}{(\rho c)_f} \frac{\partial q_r}{\partial y} + \frac{\nu_f}{(\rho c)_f} \left(\frac{\partial u}{\partial y} \right)^2 \tag{2.3}$$

$$u \frac{\partial C}{\partial x} + v \frac{\partial C}{\partial y} = D_B \frac{\partial^2 C}{\partial y^2} + \frac{D_T}{T_\infty} \frac{\partial^2 T}{\partial y^2} - k_1 C \tag{2.4}$$

The appropriate boundary conditions for the flow model are written as follows

$$\begin{aligned} u = U_w, v = 0, \frac{\partial T}{\partial y} = -h_s T, \frac{\partial C}{\partial y} = -h_c C \quad \text{at} \quad y = 0 \\ u \rightarrow 0, T \rightarrow T_\infty, C \rightarrow C_\infty \quad \text{as} \quad y \rightarrow \infty \end{aligned} \tag{2.5}$$

Since the surface be stretched with velocity Bx , thus $U_w = Bx$ and u and v are horizontal and vertical components of velocity, ν_f be kinematic viscosity, q_w, q_m are the heat and mass fluxes unit area at the surface, respectively.

B_0 be magnetic field, α_f be nanofluid thermal diffusivity, h_s be heat transfer coefficient, h_c be concentration coefficient, ρ be nanofluid density, q_0 be heat source or sink constant, $(\rho c)_f$ be heat capacities of the fluid, T be temperature, k be nanofluid thermal conductivity, D_B be Brownian diffusion coefficient, C be nanoparticle volumetric fraction, D_T be thermophoretic diffusion coefficient and T_∞ be the ambient fluid temperature.

The radiative heat flux term q_r is simplified by the Rosseland approximation and is expressed as

$$q_r = -\frac{4\sigma' \partial T^4}{3k^* \partial y} \tag{2.6}$$

Since the Rosseland approximation is valid only, optically thick fluids can be considered for the present investigation. It is assumed that the temperature differences within the flow are significantly small, then (2.6) can be linearized by expanding T^4 into the Taylor series about T_∞ and neglecting higher order terms as

$$T^4 \cong 4T_\infty^3 T - 3T_\infty^4 \tag{2.7}$$

Then, the radiation term in Equation (2.3) becomes as below

$$\frac{\partial q_r}{\partial y} = -\frac{16\sigma T_\infty^3 \partial^2 T}{3k^* \partial y^2} \tag{2.8}$$

Substituting of this equation (2.8) into the Equation (2.3), we have

$$u \frac{\partial T}{\partial x} + v \frac{\partial T}{\partial y} = \alpha_f \frac{\partial^2 T}{\partial y^2} + \tau \left[D_B \frac{\partial C}{\partial y} \frac{\partial T}{\partial y} + \frac{D_T}{T_\infty} \left(\frac{\partial T}{\partial y} \right)^2 \right] + \frac{1}{(\rho c)_f} \frac{16\sigma T_\infty^3 \partial^2 T}{3k^* \partial y^2} + \frac{\nu_f}{(\rho c)_f} \left(\frac{\partial u}{\partial y} \right)^2 \tag{2.9}$$

The equation of continuity (2.1) is satisfied for the choice of a stream function $\psi(x, y)$ such that $u = \psi_y, v = -\psi_x$

$$\tag{2.10}$$

In order to transform the equations (2.2), (2.4) and (2.9) into a set of ordinary differential equations, the following similarity transformations and dimensionless variables are introduced.

$$\psi = (av)^{\frac{1}{2}} x f(\eta), \eta = y \sqrt{\frac{a}{v}}, \theta(\eta) = \frac{T - T_\infty}{T_w - T_\infty}, \beta(\eta) = \frac{C - C_\infty}{C_w - C_\infty}$$

$$Pr = \frac{\nu_f}{\alpha_f}, M = \frac{\sigma B_0^2}{\rho a}, K = \frac{\nu_f}{k a}, Le = \frac{\nu_f}{D_B}, Nb = \frac{\tau_{DB}(C_w - C_\infty)}{\nu_f}$$

$$Nt = \frac{\tau_{DT}(T_w - T_\infty)}{T_\infty \nu_f}, \gamma = h_s \sqrt{\frac{\nu}{a}}, \beta_1 = h_c \sqrt{\frac{\nu}{a}}, kr = \frac{\nu k_1}{a}$$

$$Ec = \frac{U_w^2}{c_f(T_w - T_\infty)}, Rd = \frac{4\sigma T_\infty^3}{k^* c_f}$$

where $f(\eta)$ be dimensionless stream function, θ be dimensionless temperature, ϕ be dimensionless nanoparticle volume fraction, η be similarity variable, M be magnetic parameter, λ be non-Newtonian williamson parameter, Le be Lewis number, Nb be Brownian motion parameter, Nt be thermophoresis parameter, Ec be Eckert number, Pr be Prandtl number, γ be conjugate parameter for Newtonian heating, β_1 be conjugate parameter for concentration.

After the substitution of these transformations (2.10) – (2.11) into the equations (2.2), (2.9) and (2.4), the resulting non-linear ordinary differential equations are written as

$$f'''(\eta) + f(\eta)f''(\eta) - f'^2(\eta) + \lambda f''(\eta)f'''(\eta) - (M + K)f'(\eta) = 0 \quad (2.12)$$

$$\frac{1}{Pr} \left(1 + \frac{4}{3}Rd\right) \theta''(\eta) + f(\eta)\theta'(\eta) + Nb\theta'(\eta)\beta'(\eta) + Nt\theta'^2(\eta) + Ec f''^2(\eta) = 0 \quad (2.13)$$

$$\beta''(\eta) + Le f(\eta)\beta'(\eta) + \frac{Nt}{Nb} \theta''(\eta) - kr\beta(\eta) = 0 \quad (2.14)$$

together with the boundary conditions

$$f(\eta) = 0, f'(\eta) = 1, \theta'(\eta) = -\gamma(1 + \theta(\eta)), \beta'(\eta) = -\beta_1(1 + \beta(\eta)) \quad \text{at} \quad \eta = 0$$

$$f'(\eta) \rightarrow 0, \theta(\eta) \rightarrow 0, \beta(\eta) \rightarrow 0 \quad \text{as} \quad \eta \rightarrow \infty \quad (2.15)$$

Where the prime denote differentiation with respect to η .

The Physical quantities of interest like skin friction coefficient C_f , local Nusselt number Nu_x and local Sherwood number Sh_x are defined as

$$C_f = \frac{\tau_w}{\rho U_w^2}, \quad Nu_x = \frac{x q_w}{k(T_\infty - T_w)}, \quad Sh_x = \frac{x q_m}{D_B(C_\infty - C_w)} \quad (2.16)$$

Where the shear stress (τ_w), surface heat flux (q_w) and surface mass flux (q_m) are given by

$$\tau_w = \left[\mu \left(\frac{\partial u}{\partial y} + \frac{\Gamma}{\sqrt{2}} \left(\frac{\partial u}{\partial y} \right)^2 \right) \right]_{y=0}, \quad q_w = -k \left(\frac{\partial T}{\partial y} \right)_{y=0}, \quad q_m = -D_B \left(\frac{\partial C}{\partial y} \right)_{y=0} \quad (2.17)$$

Using the non-dimensional variables, we obtain

$$C_f(Re_x)^{1/2} = f''(0) + \frac{\lambda}{2} f''(0)^2, \quad Nu_x(Re_x)^{1/2} = -\theta'(0), \quad Sh_x(Re_x)^{1/2} = -\beta'(0) \quad (2.18)$$

Where $Re_x = \frac{x U_w(x)}{\nu}$ is the local Reynolds number.

III. Solution Of The Problem

For solving equations (2.12)–(2.14), a step by step integration method i.e. Runge–Kutta method has been applied. For carrying in the numerical integration, the equations are reduced to a set of first order differential equation. For performing this we make the following substitutions:

$$y_1 = f, y_2 = f', y_3 = f'', y_4 = \theta, y_5 = \theta', y_6 = \beta, y_7 = \beta'$$

$$y_3' = \frac{1}{(1 + \lambda y_3)} (y_2^2 - y_1 y_3 + (M + K) y_2)$$

$$y_5' = -\frac{Pr}{(1 + \frac{4}{3} Rd)} [y_1 y_5 + Nb y_5 y_7 + Nt y_5^2 + Ec y_3] \quad (3.1)$$

$$y_7' = -Le y_1 y_7 - \frac{Nt}{Nb} \left(-\frac{Pr}{(1 + \frac{4}{3} Rd)} [y_1 y_5 + Nb y_5 y_7 + Nt y_5^2 + Ec y_3] \right) + kr y_6$$

together with the boundary conditions are given by (2.15) taking the form

$$y_1(0) = 0, y_2(0) = 1, y_5(0) = -\gamma(1 + y_4(0)), y_7(0) = -\beta_1(1 + y_6(0))$$

$$y_2(\infty) \rightarrow 0, y_4(\infty) \rightarrow 0, y_6(\infty) \rightarrow 0 \quad (3.2)$$

In order to carry out the step by step integration of equations (2.9) –(2.11), Gills procedures as given in Ralston and Wilf (1960) have been used. To start the integration it is necessary to provide all the values of

$y_1, y_2, y_3, y_4, y_5, y_6$ at $\eta = 0$ from which point, the forward integration has been carried out but from the boundary conditions it is seen that the values of y_3, y_4, y_7 are not known. So we are to provide such values of

y_3, y_4, y_7 along with the known values of the other function at $\eta = 0$ as would satisfy the boundary conditions

as $\eta \rightarrow \infty$ to a prescribed accuracy after step by step integrations are performed. Since the values of y_3, y_4, y_7

which are supplied are merely rough values, some corrections have to be made in these values in order that the

boundary conditions to $\eta \rightarrow \infty$ are satisfied. These corrections in the values of y_3, y_4, y_7 are taken care of by a self-iterative procedure which can for convenience be called ‘‘Corrective procedure’’.

IV. Results And Discussion

In order to acquire physical understanding, the velocity, temperature & concentration distributions have been illustrated by varying the numerical values of the various parameters demonstrated in the present problem. The numerical results are tabulated and exhibited with the graphical illustration. Figures 1(a), 1(b) & 1(c) respectively, demonstrate the different values of magnetic parameter (M) on dimensionless velocity, temperature and concentration profiles. The values of M is taken to be M = 0, 2, 3, 6 and the other parameters are kept constant at K = 0.2, $\lambda = 0.2$, Pr = 4, Nt = 0.1, Nb = 0.1, Le = 4, Ec = 0.1, kr = 0.5, Rd = 1, $\gamma = 0.2$ & $\beta_1 = 0.2$. It is noticed that, with the hype in the values of M from 0 to 6 then the velocity significantly decreases consequently decreases the thickness of momentum boundary layer but the temperature and concentration of the fluid increases. This is due to the fact that, the introduction of transverse magnetic field has a tendency to create a drag, known as the Lorentz force which tends to resist the flow.

Figures 2(a), 2(b) & 2(c) establish the different values of permeability of the porous medium parameter (K) on velocity, temperature and concentration profiles, respectively. The values of K is taken to be K = 0, 0.5, 1, 2 and the other parameters are kept constant at M = 0.5, $\lambda = 0.2$, Pr = 4, Nt = 0.1, Nb = 0.1, Le = 4, Ec = 0.1, kr = 0.5, Rd = 1, $\gamma = 0.2$ & $\beta_1 = 0.2$. It is noticed that, with the hype in the values of K from 0 to 2 then the velocity decreases consequently decreases the thickness of momentum boundary layer but the temperature and concentration of the fluid increases. The reason for this, the porous medium obstructs the fluid to move freely through the boundary layer. This leads to the raise in the thickness of thermal and concentration boundary layer. Figures 3(a), 3(b) & 3(c) illustrate the effect of non-Newtonian williamson parameter (λ) on velocity, temperature and concentration profiles, respectively. The values of λ is taken to be $\lambda = 0, 0.1, 0.2, 0.3$ and by setting the values of other parameters to be constant at for K = 0.2, M = 0.5, Pr = 4, Nt = 0.1, Nb = 0.1, Le = 4, Ec = 0.1, kr = 0.5, Rd = 1, $\gamma = 0.2$ & $\beta_1 = 0.2$. From these figures it is observed that as λ raises from 0 to 2, the velocity remarkably decreases. While the non-Newtonian Williamson parameter increases, the temperature profile is increased. This fact is illustrated in figure 3(b). In the concentration profile, increase the value of λ result in a significant increase in the boundary layer thickness, which is shown in figure 3(c). The phenomenon in which the particles can diffuse under the effect of a temperature gradient is called thermophoresis. The influence of thermophoresis parameter (Nt) on the temperature and concentration fields is shown in figures 4(a) and 4(b) respectively. The values of Nt is taken to be Nt = 0.1, 0.2, 0.3, 0.4 and the other parameters are fixed as K = 0.2, M = 0.5, $\lambda = 0.2$, Pr = 4, Nb = 0.1, Le = 4, Ec = 0.1, kr = 0.5, Rd = 1, $\gamma = 0.2$ & $\beta_1 = 0.2$. It is conformed that enhances the values of Nt from 0.1 to 0.4, the temperature & concentration of the fluid increases. This leads to enhance the thickness of thermal and concentration boundary layer. The random motion of nanoparticles within the base fluid is called Brownian motion which occurs due to the continuous collisions between the nanoparticles and the molecules of the base fluid. The effect of Brownian motion parameter (Nb) on the temperature and concentration fields is illustrated in figures 5(a) & 5(b) respectively. The values of Nb is taken to be Nb = 0.1, 0.2, 0.3, 0.4 and the other parameters are fixed as K = 0.2, M = 0.5, $\lambda = 0.2$, Pr = 4, Nt = 0.1, Le = 4, Ec = 0.1, kr = 0.5, Rd = 1, $\gamma = 0.2$ & $\beta_1 = 0.2$. It is conformed that enhances the values of Nb from 0.1 to 0.4, the temperature profile significantly increases but concentration decreases. In the system nanofluid, the Brownian motion takes a place in the presence of nanoparticles. When hype the values of Nb, the Brownian motion is affected and the concentration boundary layer thickness reduces and accordingly the heat transfer characteristics of the fluid changes.

The effect of Eckert number (Ec) on temperature and concentration fields is depicted in figures 6(a) and 6(b), respectively. The values of Ec is taken to be Ec = 0.1, 0.5, 1, 1.5 and the other parameters are fixed as K = 0.2, M = 0.5, $\lambda = 0.2$, Pr = 4, Nt = 0.1, Nb = 0.1, Le = 4, kr = 0.5, Rd = 1, $\gamma = 0.2$ & $\beta_1 = 0.2$. It is observed that the thickness of thermal and concentration boundary layer significantly increases with raising the values of Ec from 0.1 to 1.5. For the constant parameters K = 0.2, M = 0.5, $\lambda = 0.2$, Pr = 4, Nt = 0.1, Nb = 0.1, Le = 4, Ec = 0.1, kr = 0.5, $\gamma = 0.2$ & $\beta_1 = 0.2$, Figures 7(a) & 7(b) illustrate the effect of radiation parameter (Rd) in the presence of viscous dissipation on the dimensionless temperature and nanoparticle volume fraction profiles. From figures 7(a) & 7(b), it can be understood that thermal and concentration boundary layer thickness increases with an increase in thermal radiation. Therefore higher values of radiation parameter imply higher surface heat flux which will increase the temperature within the boundary layer region. Figures 8(a) and 8(b) depicts the various values of conjugate parameter for Newtonian heating (γ) on the dimensionless temperature and concentration profiles, respectively. The values of γ is taken to be $\gamma = 0, 0.1, 0.2, 0.3$ and the other parameters are fixed as K = 0.2, M = 0.5, $\lambda = 0.2$, Pr = 4, Nt = 0.1, Nb = 0.1, Le = 4, Ec = 0.1, kr = 0.5, Rd = 1 & $\beta_1 = 0.2$. It can be understood that raising the values of γ from 0.1 to 0.4 the resultant temperature and concentration increases consequently thickness of thermal and concentration boundary layer enhances.

Figures 9(a) and 9(b) depicts the various values of conjugate parameter for concentration (β_1) on the temperature and concentration fields, respectively. The values of β_1 is taken to be $\beta_1 = 0, 0.3, 0.5, 0.8$ and the other parameters are fixed as $K = 0.2, M = 0.5, \lambda = 0.2, Pr = 4, Nt = 0.1, Nb = 0.1, Le = 4, Ec = 0.1, kr = 0.5, Rd = 1$ & $\gamma = 0.2$. It is obtained that raising the values of β from 0.1 to 1.0, the resulting dimensionless temperature and concentration of the fluid increases. This leads to enhance the thermal and concentration boundary layer thickness. The effect of Prandtl number Pr on dimensionless temperature fields is shown in figures 10 respectively. The values of Pr is taken to be $Pr = 4, 6, 8, 10$ and the other parameters are fixed as $K = 0.2, M = 0.5, \lambda = 0.2, Nt = 0.1, Nb = 0.1, Le = 4, Ec = 0.1, kr = 0.5, Rd = 1, \gamma = 0.2$ & $\beta_1 = 0.2$. Physically, increasing Prandtl number becomes a key factor to reduce the thickness of thermal boundary layer. The effect of Lewis number Le verses concentration profile is shown in figure 11 respectively. The values of Le is taken to be $Le = 4, 6, 8, 10$ and the other parameters are fixed as $K = 0.2, M = 0.5, \lambda = 0.2, Pr = 4, Nt = 0.1, Nb = 0.1, Ec = 0.1, kr = 0.5, Rd = 1, \gamma = 0.2$ & $\beta_1 = 0.2$. It can be obtained that the concentration of the fluid decreases with raising the values of Le from 4 to 10. The effect of chemical reaction parameter (kr) verses concentration profile is shown in figure 12 respectively. The values of kr is taken to be $kr = 0, 0.5, 1, 2$ and the other parameters are fixed as $K = 0.2, M = 0.5, \lambda = 0.2, Pr = 4, Nt = 0.1, Nb = 0.1, Le = 4, Ec = 0.1, Rd = 1, \gamma = 0.2$ & $\beta_1 = 0.2$. It can be obtained that the concentration of the fluid decreases with raising the values of kr from 0 to 2.

In order to standardize the method used in the present study and to decide the accuracy of the present analysis and to compare with the results available (Nadeem and Hussain (2013), Khan and Pop (2010), Gorla and Sidawi (1994) and Wang (1989)) relating to the local Nusselt number, and found in an agreement (Table.1).

Table 1 Shows that magnitude of skin-friction coefficient $\left| f''(0) + \frac{\lambda}{2} f''(0)^2 \right|$, local Nusselt number $-\theta'(0)$ and local Sherwood number $-\beta'(0)$ on $M, K, \lambda, Pr, Nt, Nb, K, Ec, kr, Rd, \gamma$ and β , respectively. As M increases from 0.5 to 2 then $\left| f''(0) + \frac{\lambda}{2} f''(0)^2 \right|, -\theta'(0)$ and $-\beta'(0)$ increases. As K increases from 0.2 to 3 then $\left| f''(0) + \frac{\lambda}{2} f''(0)^2 \right|, -\theta'(0)$ and $-\beta'(0)$ increases. As λ increases from 0.2 to 0.4 then $\left| f''(0) + \frac{\lambda}{2} f''(0)^2 \right|, -\theta'(0)$ and $-\beta'(0)$ increases. As Pr increases from 4 to 15 then $-\theta'(0)$ and $-\beta'(0)$ decreases. As Nt increases from 0.1 to 2 then $\left| f''(0) + \frac{\lambda}{2} f''(0)^2 \right|$ increases $-\theta'(0)$ decreases and $-\beta'(0)$ increases. As Nb increases from 0.1 to 2 then $\left| f''(0) + \frac{\lambda}{2} f''(0)^2 \right|, -\theta'(0)$ and $-\beta'(0)$ increases. As Le increases from 4 to 10 then $-\theta'(0)$ and $-\beta'(0)$ decreases. As kr increases from 0.1 to 2 then $\left| f''(0) + \frac{\lambda}{2} f''(0)^2 \right|$ increases $-\theta'(0)$ decreases and $-\beta'(0)$ increases. As Ec increases from 0.1 to 1.5 then $-\theta'(0)$ increases and $-\beta'(0)$ decreases. As Rd increases from 1 to 4 then $\left| f''(0) + \frac{\lambda}{2} f''(0)^2 \right|, -\theta'(0)$ and $-\beta'(0)$ increases. As γ increases from 0.2 to 0.5 then $\left| f''(0) + \frac{\lambda}{2} f''(0)^2 \right|, -\theta'(0)$ and $-\beta'(0)$ increases. As β_1 increases from 0.2 to 0.8 then $-\theta'(0)$ and $-\beta'(0)$ increases.

V. Conclusions

In this paper numerically investigated radiation and chemical reaction effects on the steady boundary layer flow of MHD Williamson fluid through porous medium toward a horizontal linearly stretching sheet in the presence of nanoparticles in the presence of viscous dissipation and Newtonian heating. The important findings of the paper are:

- The velocity of the fluid decreases with an increase of the Non-Newtonian Williamson parameter or magnetic parameter or permeability parameter. The fluid temperature and concentration increases with the influence of non-Newtonian Williamson parameter or magnetic parameter or permeability parameter.
- The temperature and concentration enhance with the raising the values of Eckert number or radiation parameter or conjugate parameter for Newtonian heating or conjugate parameter for concentration.
- Both the local Nusselt number and local Sherwood number decreases with the raising the values of non-Newtonian Williamson parameter or magnetic parameter.

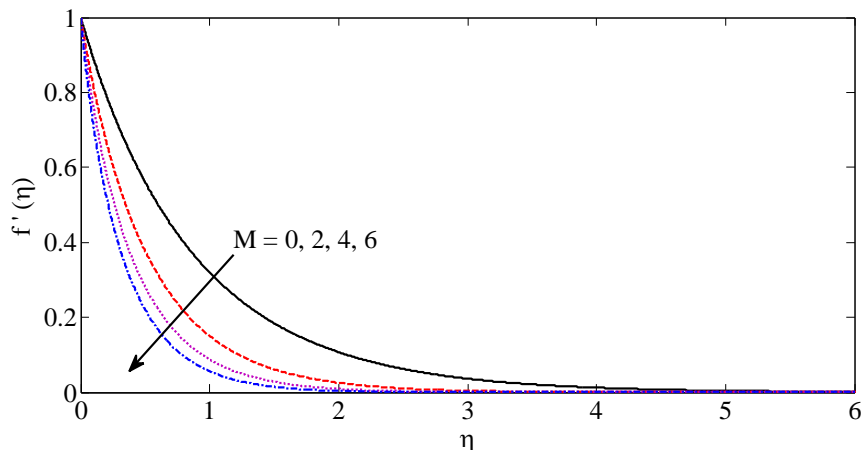


Fig.1(a) Velocity for a range of values of M with $K = 0.2, \lambda = 0.2, Pr = 4, Nt = 0.1, Nb = 0.1, Le = 4, Ec = 0.1, kr = 0.5, Rd = 1, \gamma = 0.2$ & $\beta_1 = 0.2$.

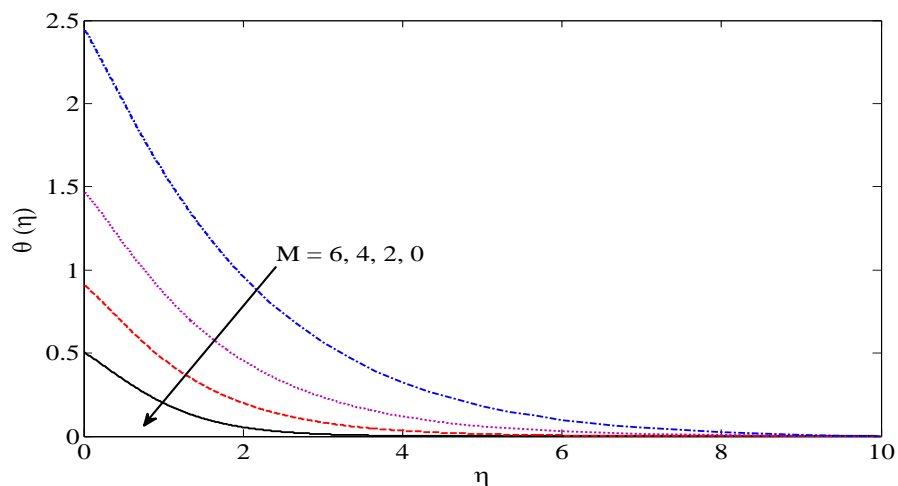


Fig.1(b) Temperature for a range of values of M with $K = 0.2, \lambda = 0.2, Pr = 4, Nt = 0.1, Nb = 0.1, Le = 4, Ec = 0.1, kr = 0.5, Rd = 1, \gamma = 0.2$ & $\beta_1 = 0.2$.

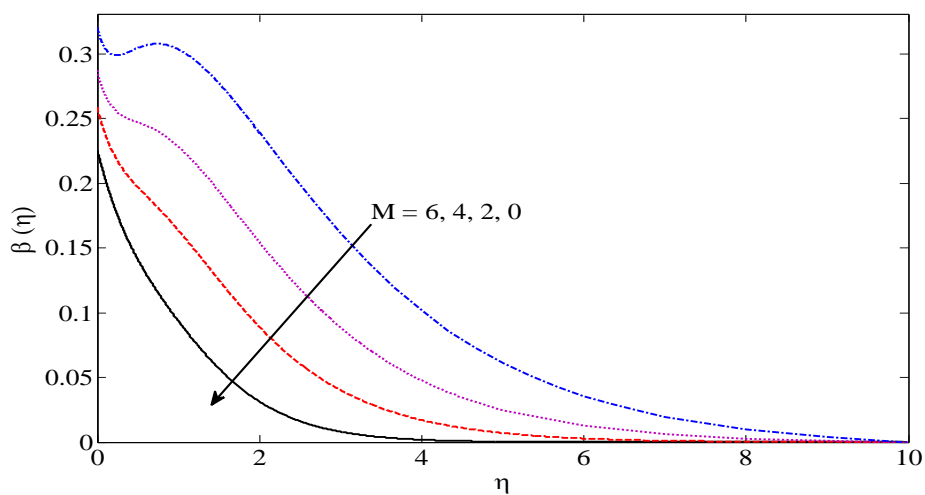


Fig.1(c) Nanoparticle volume fraction for a range of values of M with $K = 0.2, \lambda = 0.2, Pr = 4, Nt = 0.1, Nb = 0.1, Le = 4, Ec = 0.1, kr = 0.5, Rd = 1, \gamma = 0.2$ & $\beta_1 = 0.2$.

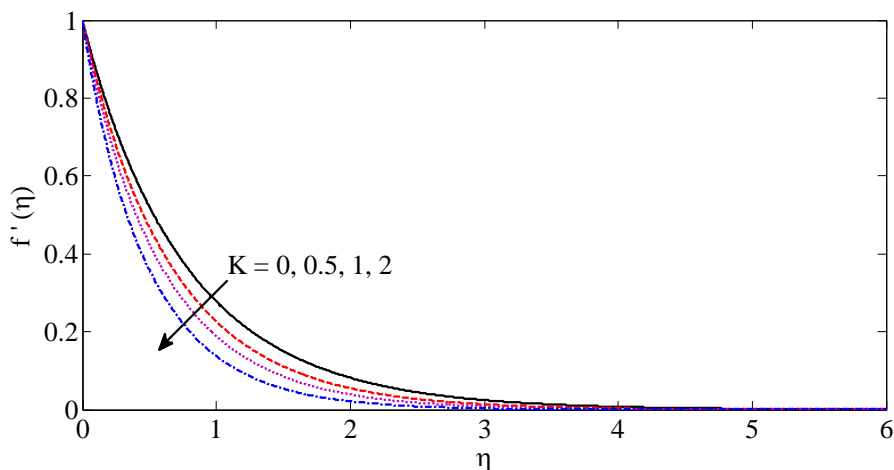


Fig.2 (a) Velocity for a range of values of K with $M = 0.5, \lambda = 0.2, Pr = 4, Nt = 0.1, Nb = 0.1, Le = 4, Ec = 0.1, kr = 0.5, Rd = 1, \gamma = 0.2$ & $\beta_1 = 0.2$.

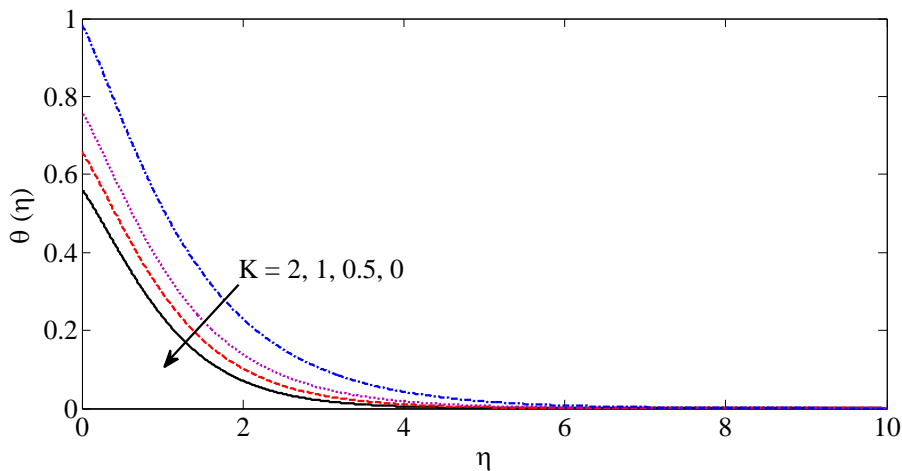


Fig.2(b) Temperature for a range of values of K with $M = 0.5, \lambda = 0.2, Pr = 4, Nt = 0.1, Nb = 0.1, Le = 4, Ec = 0.1, kr = 0.5, Rd = 1, \gamma = 0.2$ & $\beta_1 = 0.2$.

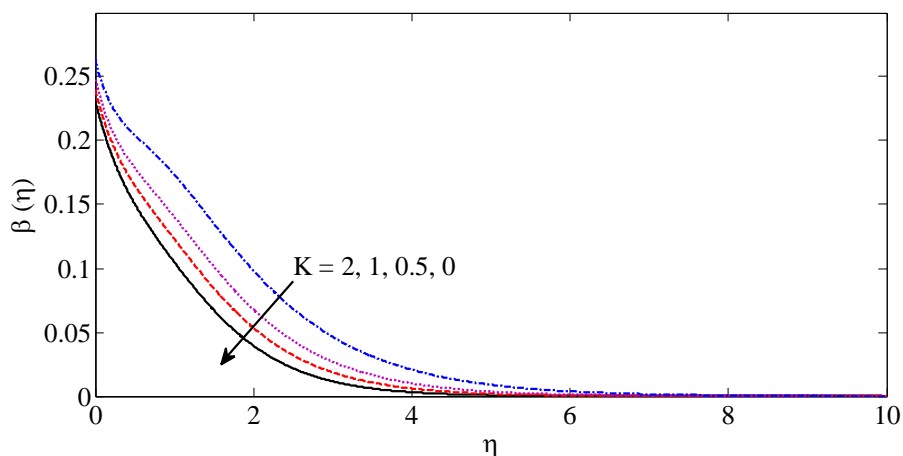


Fig.2(c) Nanoparticle volume fraction for a range of values of K with $M = 0.5, \lambda = 0.2, Pr = 4, Nt = 0.1, Nb = 0.1, Le = 4, Ec = 0.1, kr = 0.5, Rd = 1, \gamma = 0.2$ & $\beta_1 = 0.2$.

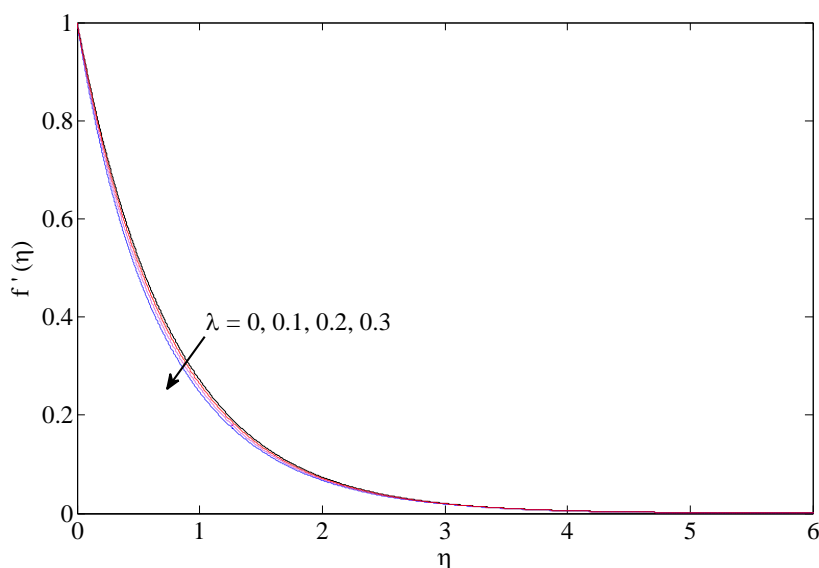


Fig.3(a) Velocity for a range of values of λ with $K = 0.2, M = 0.5, Pr = 4, Nt = 0.1, Nb = 0.1, Le = 4, Ec = 0.1, kr = 0.5, Rd = 1, \gamma = 0.2$ & $\beta_1 = 0.2$.

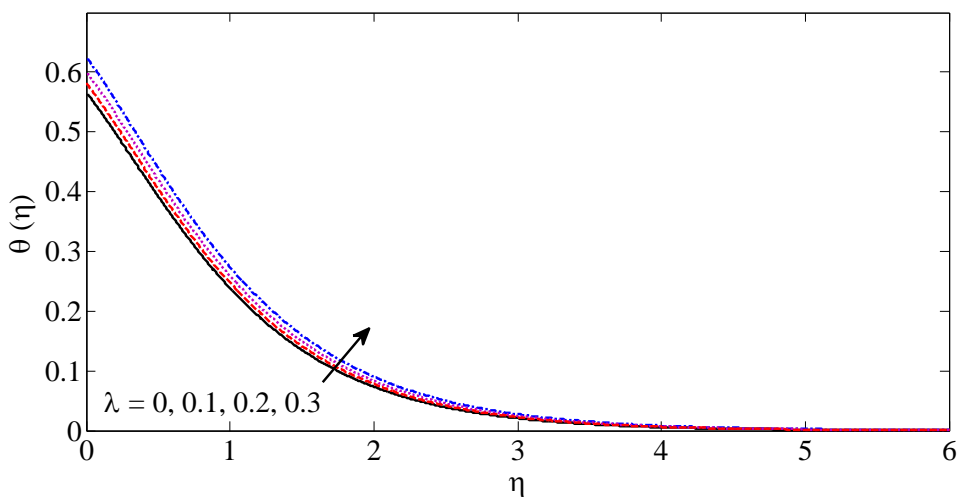


Fig.3(b) Temperature for a range of values of λ with $K = 0.2, M = 0.5, Pr = 4, Nt = 0.1, Nb = 0.1, Le = 4, Ec = 0.1, kr = 0.5, Rd = 1, \gamma = 0.2$ & $\beta_1 = 0.2$.

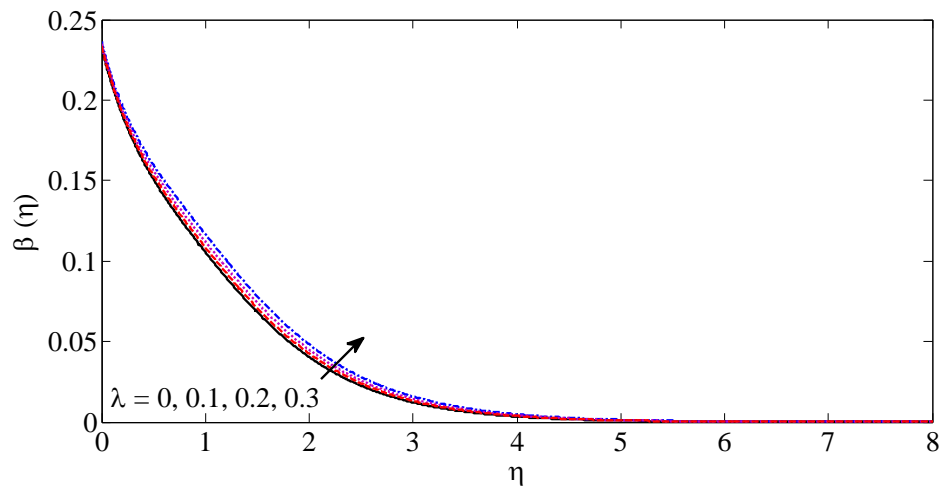


Fig.3(c) Nanoparticle volume fraction for a range of values of λ with $K = 0.2, M = 0.5, Pr = 4, Nt = 0.1, Nb = 0.1, Le = 4, Ec = 0.1, kr = 0.5, Rd = 1, \gamma = 0.2$ & $\beta_1 = 0.2$.

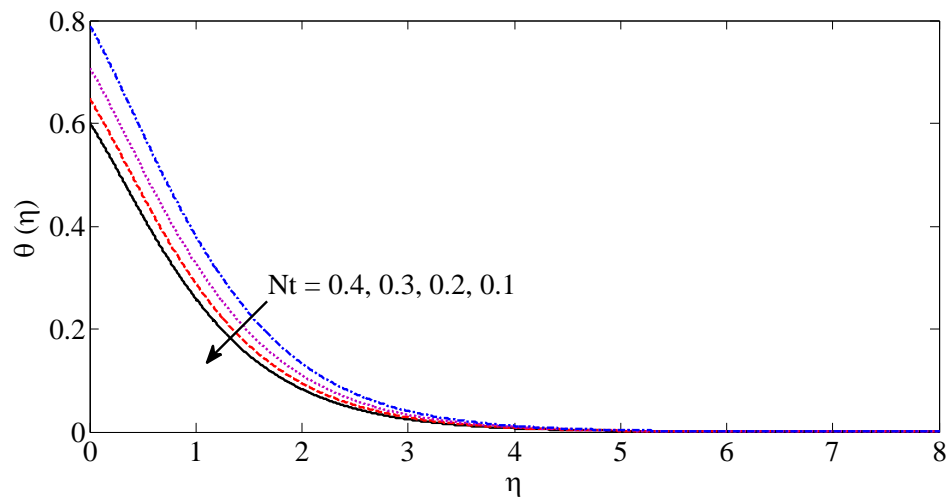


Fig.4(a) Temperature for a range of values of Nt with $K = 0.2, M = 0.5, \lambda = 0.2, Pr = 4, Nb = 0.1, Le = 4, Ec = 0.1, kr = 0.5, Rd = 1, \gamma = 0.2$ & $\beta_1 = 0.2$.

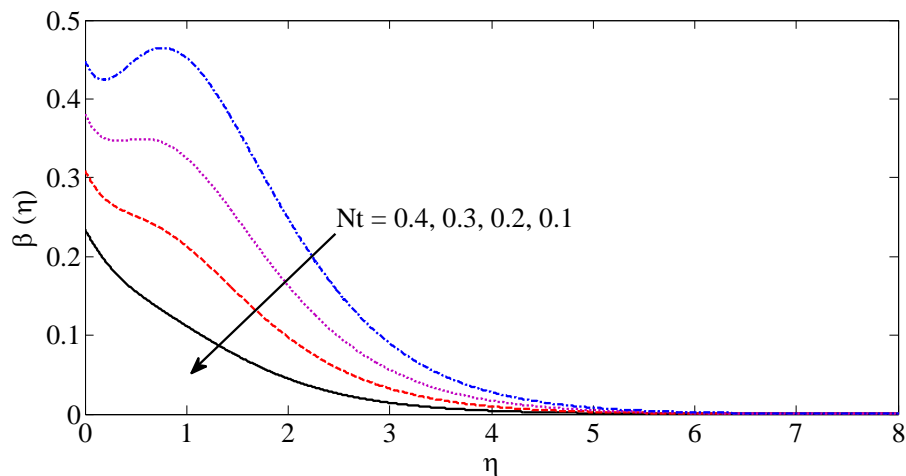


Fig.4(b) Nanoparticle volume fraction for a range of values of Nt with $K = 0.2, M = 0.5, \lambda = 0.2, Pr = 4, Nb = 0.1, Le = 4, Ec = 0.1, kr = 0.5, Rd = 1, \gamma = 0.2$ & $\beta_1 = 0.2$.

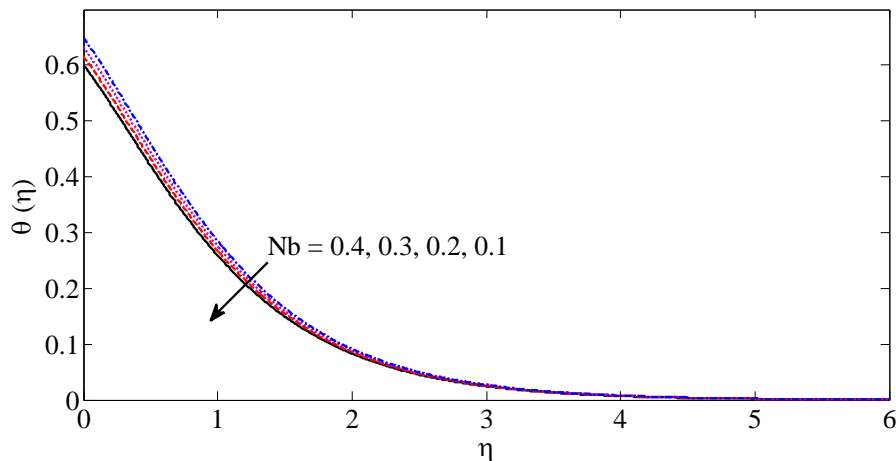


Fig.5(a) Temperature for a range of values of Nb with $K = 0.2, M = 0.5, \lambda = 0.2, Pr = 4, Nt = 0.1, Le = 4, Ec = 0.1, kr = 0.5, Rd = 1, \gamma = 0.2$ & $\beta_1 = 0.2$.

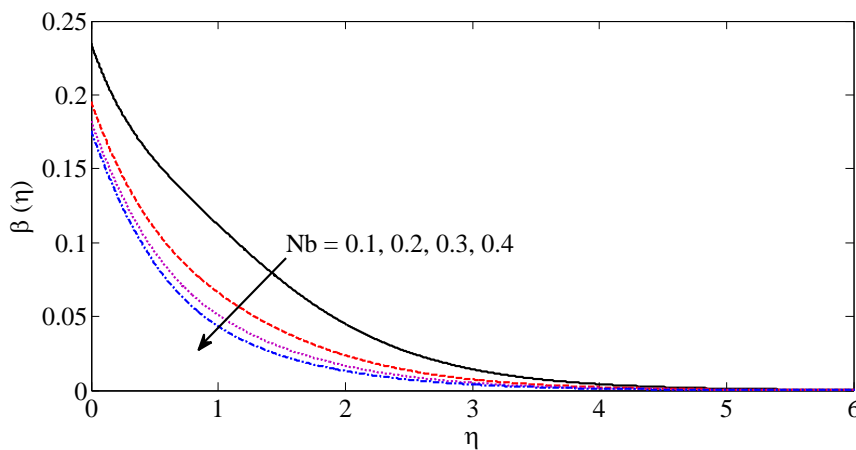


Fig.5(b) Nanoparticle volume fraction for a range of values of Nb with $K = 0.2, M = 0.5, \lambda = 0.2, Pr = 4, Nt = 0.1, Le = 4, Ec = 0.1, kr = 0.5, Rd = 1, \gamma = 0.2$ & $\beta_1 = 0.2$.

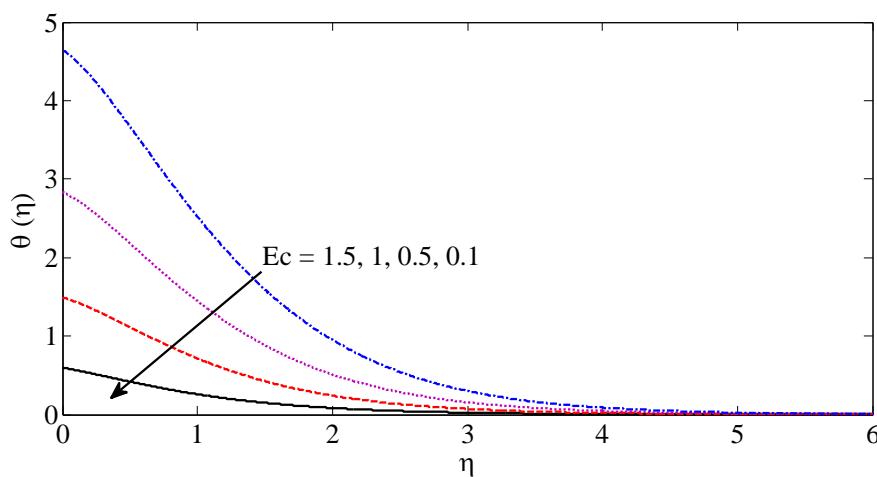


Fig.6(a) Temperature for a range of values of Ec with $K = 0.2, M = 0.5, \lambda = 0.2, Pr = 4, Nt = 0.1, Nb = 0.1, Le = 4, kr = 0.5, Rd = 1, \gamma = 0.2$ & $\beta_1 = 0.2$.

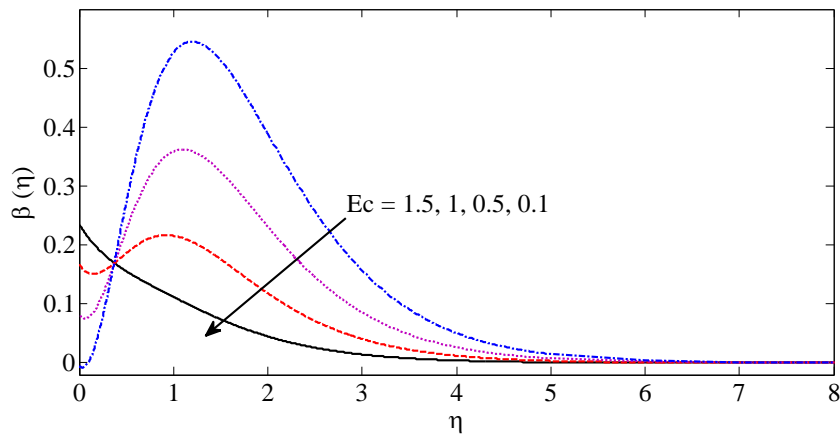


Fig.6(b) Nanoparticle volume fraction for a range of values of Ec with $K = 0.2, M = 0.5, \lambda = 0.2, Pr = 4, Nt = 0.1, Nb = 0.1, Le = 4, kr = 0.5, Rd = 1, \gamma = 0.2$ & $\beta_1 = 0.2$.

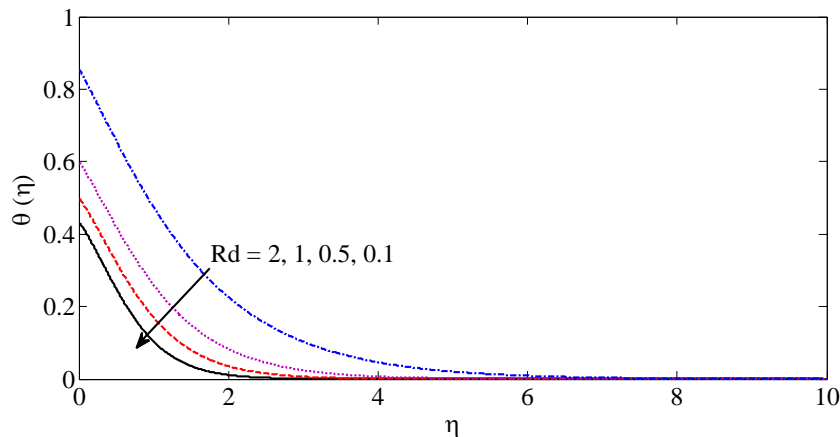


Fig.7(a) Temperature for a range of values of Rd with $K = 0.2, M = 0.5, \lambda = 0.2, Pr = 4, Nt = 0.1, Nb = 0.1, Le = 4, Ec = 0.1, kr = 0.5, \gamma = 0.2$ & $\beta_1 = 0.2$.

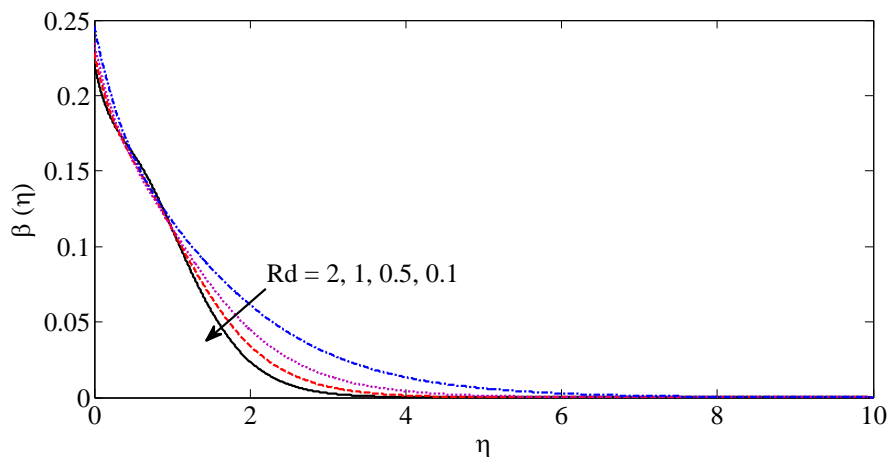


Fig.7(b) Nanoparticle volume fraction for a range of values of Rd with $K = 0.2, M = 0.5, \lambda = 0.2, Pr = 4, Nt = 0.1, Nb = 0.1, Le = 4, Ec = 0.1, kr = 0.5, \gamma = 0.2$ & $\beta_1 = 0.2$.

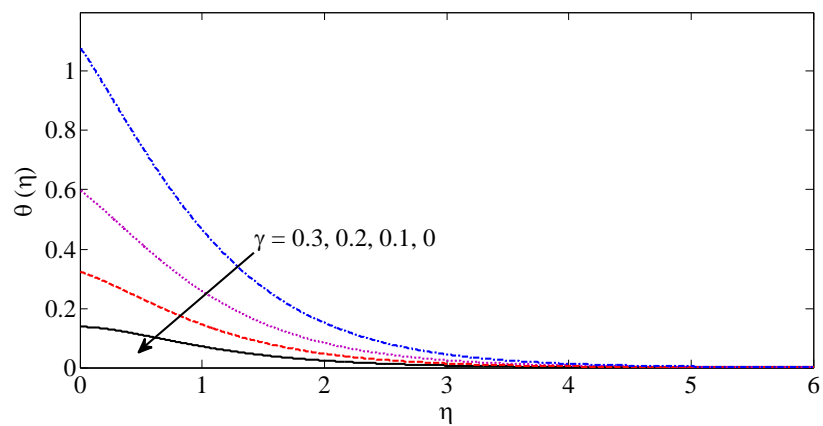


Fig.8(a) Temperature for a range of values of γ with $K = 0.2, M = 0.5, \lambda = 0.2, Pr = 4, Nt = 0.1, Nb = 0.1, Le = 4, Ec = 0.1, kr = 0.5, Rd = 1$ & $\beta_1 = 0.2$.

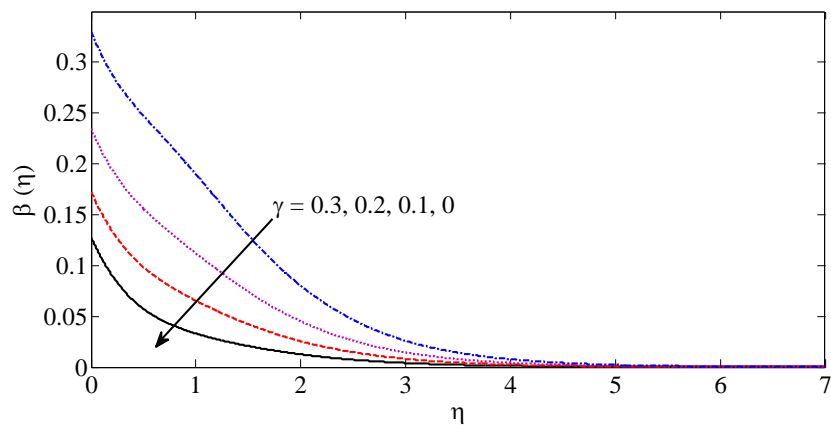


Fig.8(b) Nanoparticle volume fraction for a range of values of γ with $K = 0.2, M = 0.5, \lambda = 0.2, Pr = 4, Nt = 0.1, Nb = 0.1, Le = 4, Ec = 0.1, kr = 0.5, Rd = 1$ & $\beta_1 = 0.2$.

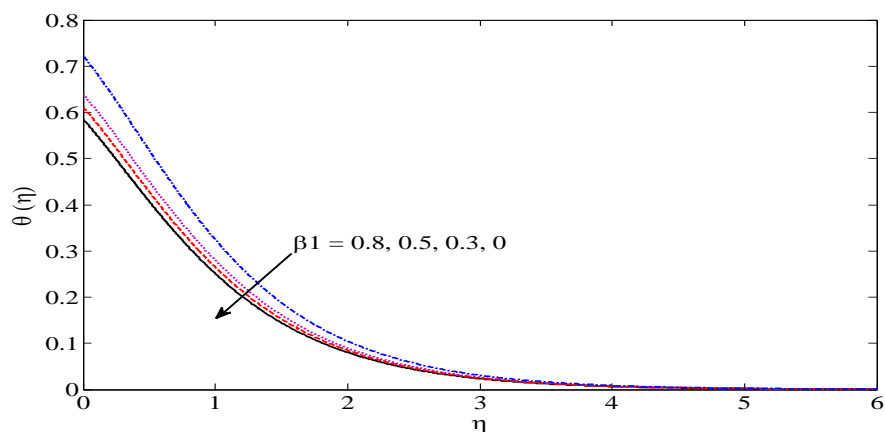


Fig.9(a) Temperature for a range of values of β_1 with $K = 0.2, M = 0.5, \lambda = 0.2, Pr = 4, Nt = 0.1, Nb = 0.1, Le = 4, Ec = 0.1, kr = 0.5, Rd = 1$ & $\gamma = 0.2$.

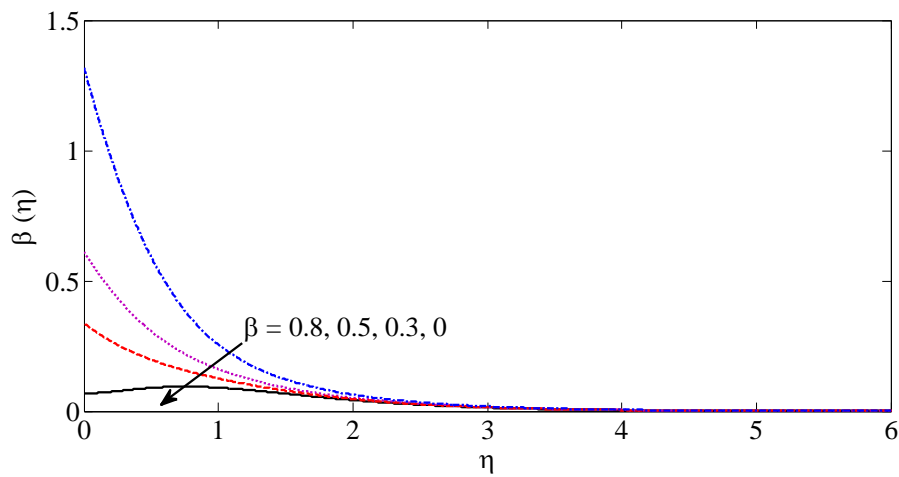


Fig.9(b) Nanoparticle volume fraction for a range of values of β_1 with $K = 0.2, M = 0.5, \lambda = 0.2, Pr = 4, Nt = 0.1, Nb = 0.1, Le = 4, Ec = 0.1, kr = 0.5, Rd = 1$ & $\gamma = 0.2$.

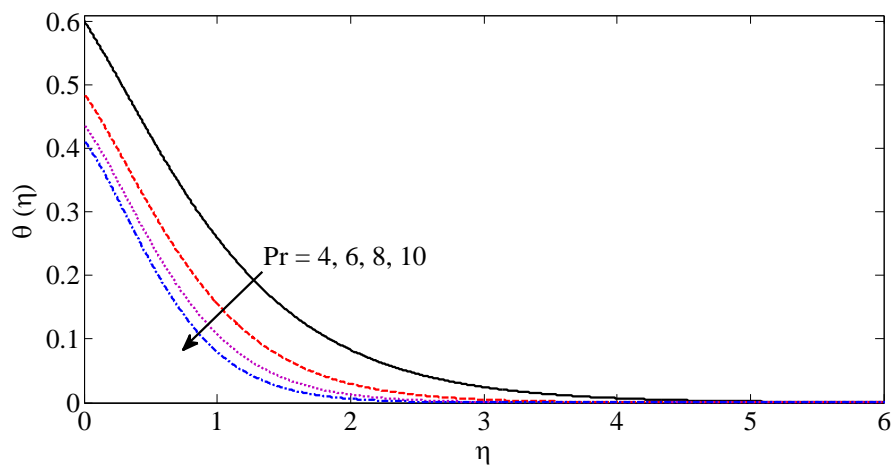


Fig.10 Temperature for a range of values of Pr with $K = 0.2, M = 0.5, \lambda = 0.2, Nt = 0.1, Nb = 0.1, Le = 4, Ec = 0.1, kr = 0.5, Rd = 1, \gamma = 0.2$ & $\beta_1 = 0.2$.

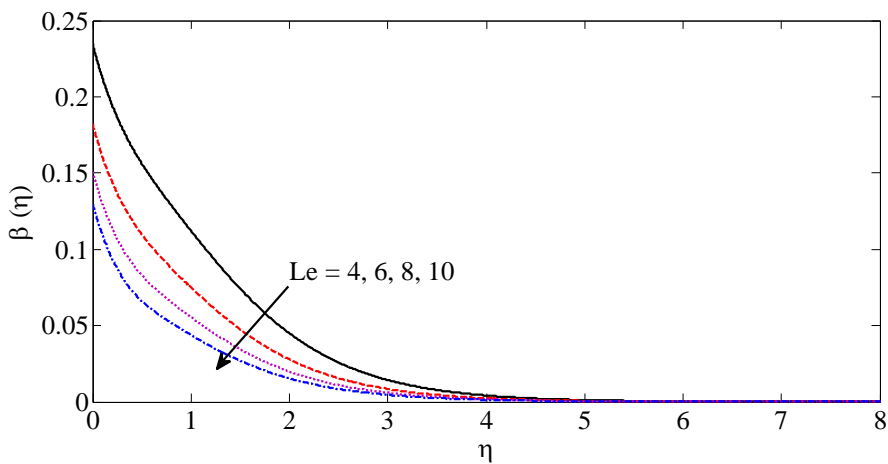


Fig.11 Nanoparticle volume fraction for a range of values of Le with $K = 0.2, M = 0.5, \lambda = 0.2, Pr = 4, Nt = 0.1, Nb = 0.1, Ec = 0.1, kr = 0.5, Rd = 1, \gamma = 0.2$ & $\beta_1 = 0.2$.

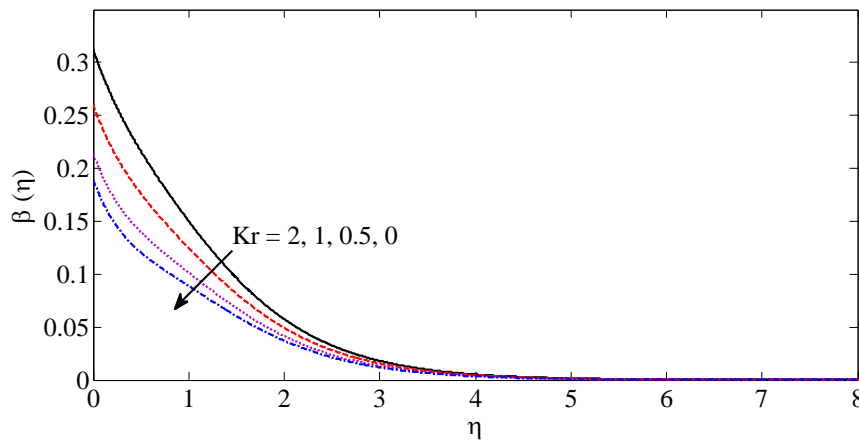


Fig.12 Nanoparticle volume fraction for a range of values of Kr with K = 0.2, M = 0.5, λ = 0.2, Pr = 4, Nt = 0.1, Nb = 0.1, Le = 4, Ec = 0.1, Rd = 1, γ = 0.2 & β₁ = 0.2.

Table 1 Comparison for viscous case $-\theta'(0)$ with Pr for $\beta_1 = Nt = Nb = Le = Ec = \gamma = 0$

Pr	$-\theta'(0)$				
	Present results	Nadeem and Hussain (2013)	Khan and Pop (2010)	Golra and Sidawi (1994)	Wang (1989)
0.07	0.066000	0.066	0.066	0.066	0.066
0.2	0.169522	0.169	0.169	0.169	0.169
0.7	0.453916	0.454	0.454	0.454	0.454
2.0	0.911358	0.911	0.911	0.911	0.911

Table 2 Computations for viscous case $f''(0) + \frac{\lambda}{2} f''(0)^2, -\theta'(0), -\phi'(0)$.

M	K	λ	Pr	Nt	Nb	Le	Ec	kr	Rd	γ	β ₁	$ f''(0) + \frac{\lambda}{2} f''(0)^2 $	$-\theta'(0)$	$-\phi'(0)$
0.5	0.2	0.2	4	0.1	0.1	4	0.1	0.5	1	0.2	0.2	1.591756	0.320242	0.246938
1	0.2	0.2	4	0.1	0.1	4	0.1	0.5	1	0.2	0.2	1.847134	0.339726	0.248637
1.5	0.2	0.2	4	0.1	0.1	4	0.1	0.5	1	0.2	0.2	2.086002	0.360433	0.250235
2	0.2	0.2	4	0.1	0.1	4	0.1	0.5	1	0.2	0.2	2.314595	0.382684	0.251752
0.5	1	0.2	4	0.1	0.1	4	0.1	0.5	1	0.2	0.2	1.991975	0.357983	0.249607
0.5	2	0.2	4	0.1	0.1	4	0.1	0.5	1	0.2	0.2	2.448619	0.396916	0.252632
0.5	3	0.2	4	0.1	0.1	4	0.1	0.5	1	0.2	0.2	2.888542	0.450381	0.255460
0.5	0.2	0.3	4	0.1	0.1	4	0.1	0.5	1	0.2	0.2	1.799737	0.325142	0.247232
0.5	0.2	0.35	4	0.1	0.1	4	0.1	0.5	1	0.2	0.2	1.941639	0.328266	0.247391
0.5	0.2	0.4	4	0.1	0.1	4	0.1	0.5	1	0.2	0.2	2.144219	0.330157	0.247552
0.5	0.2	0.2	8	0.1	0.1	4	0.1	0.5	1	0.2	0.2	1.591756	0.287677	0.244286
0.5	0.2	0.2	12	0.1	0.1	4	0.1	0.5	1	0.2	0.2	1.591756	0.279773	0.242471
0.5	0.2	0.2	15	0.1	0.1	4	0.1	0.5	1	0.2	0.2	1.591756	0.277448	0.241276
0.5	0.2	0.2	4	0.5	0.1	4	0.1	0.5	1	0.2	0.2	1.591756	0.384095	0.301913
0.5	0.2	0.2	4	1	0.1	4	0.1	0.5	1	0.2	0.2	1.591758	0.318626	0.353644
0.5	0.2	0.2	4	2	0.1	4	0.1	0.5	1	0.2	0.2	1.591758	0.220007	0.461285
0.5	0.2	0.2	4	0.1	0.5	4	0.1	0.5	1	0.2	0.2	1.591756	0.384095	0.301913
0.5	0.2	0.2	4	0.1	1	4	0.1	0.5	1	0.2	0.2	1.591758	0.318626	0.353644
0.5	0.2	0.2	4	0.1	2	4	0.1	0.5	1	0.2	0.2	1.591758	0.220007	0.461285
0.5	0.2	0.2	4	0.1	0.1	6	0.1	0.5	1	0.2	0.2	1.591756	0.319766	0.236435
0.5	0.2	0.2	4	0.1	0.1	8	0.1	0.5	1	0.2	0.2	1.591756	0.319436	0.230139
0.5	0.2	0.2	4	0.1	0.1	10	0.1	0.5	1	0.2	0.2	1.591756	0.319195	0.225934
0.5	0.2	0.2	4	0.1	0.1	4	0.5	0.5	1	0.2	0.2	1.591756	0.499045	0.233489
0.5	0.2	0.2	4	0.1	0.1	4	1	0.5	1	0.2	0.2	1.591756	0.767406	0.216452
0.5	0.2	0.2	4	0.1	0.1	4	1.5	0.5	1	0.2	0.2	1.591756	1.130397	0.199233
0.5	0.2	0.2	4	0.1	0.1	4	0.1	1	1	0.2	0.2	1.591756	0.319670	0.237811
0.5	0.2	0.2	4	0.1	0.1	4	0.1	1.5	1	0.2	0.2	1.591756	0.319305	0.231857
0.5	0.2	0.2	4	0.1	0.1	4	0.1	2	1	0.2	0.2	1.591756	0.319054	0.227687
0.5	0.2	0.2	4	0.1	0.1	4	0.1	0.5	2	0.2	0.2	1.591756	0.371225	0.249193
0.5	0.2	0.2	4	0.1	0.1	4	0.1	0.5	3	0.2	0.2	1.591756	0.442514	0.251862
0.5	0.2	0.2	4	0.1	0.1	4	0.1	0.5	4	0.2	0.2	1.591756	0.547071	0.255556
0.5	0.2	0.2	4	0.1	0.1	4	0.1	0.5	1	0.3	0.2	1.591756	0.625034	0.266098
0.5	0.2	0.2	4	0.1	0.1	4	0.1	0.5	1	0.4	0.2	1.591756	1.494756	0.313069

0.5	0.2	0.2	4	0.1	0.1	4	0.1	0.5	1	0.5	0.2	1.591758	8.727811	0.693351
0.5	0.2	0.2	4	0.1	0.1	4	0.1	0.5	1	0.2	0.4	1.591756	0.324790	0.585077
0.5	0.2	0.2	4	0.1	0.1	4	0.1	0.5	1	0.2	0.6	1.591756	0.331900	1.076283
0.5	0.2	0.2	4	0.1	0.1	4	0.1	0.5	1	0.2	0.8	1.591756	0.344573	1.854474

References

- [1] Buongiorno, J., (2006), Convective transport in nanofluids, *Journal of heat transfer*, Vol. 128, No.3, pp.240-250.
- [2] Choi SUS, Zhang, ZG, Yu, W., Lockwood, F.E & Gruike, EA, (2001), Anomalously thermal conductivity enhancement in nano tube suspensions, *Applied Physics Letters*, Vol.79, No.14, pp.2252-2254.
- [3] Choi, S. U. S., (1995) "Enhancing thermal conductivity of fluids with nanoparticles in developments and applications of non-Newtonian flows," ASME, FED-vol. 231/MD- vol. 66, pp. 99-105.
- [4] Das M., Mahato, R., Nandkeolyar, R., (2015), Newtonian heating effect on unsteady hydromagnetic Casson fluid flow past a flat plate with heat and mass transfer, *Alexandria Engineering Journal*, Vol.54, pp.871–879.
- [5] Gorla, R.S.R., and Sidawi, I., (1994), Free convection on a vertical stretching surface with suction and blowing, *Appl Sci Res*, Vol.52, pp.247-257.
- [6] Hussanan, A. Khan, I. Shafie, S., (2013), An exact analysis of heat and mass transfer past a vertical plate with Newtonian heating, *J. Appl. Math.*, Article ID: 434571.
- [7] Hussanan, A., Salleh, M.Z., Tahar, R.M. Khan, I., (2014), Unsteady boundary layer flow and heat transfer of a Casson fluid past an oscillating vertical plate with Newtonian heating, *PloS One.*, Vol. 9(10), e108763.
- [8] Khan, W.A., and Pop, I., (2010), Boundary-layer flow of a nanofluid past a stretching sheet, *Int J Heat Mass Transf*, Vol. 53, pp.2477-2483.
- [9] Merkin, J.H., (1994), Natural-convection boundary-layer flow on a vertical surface with Newtonian heating, *Int. J. Heat Fluid Flow*, Vol.15 (5), pp.392–398.
- [10] Nadeem, S., and Hussain, S. T., (2013), Flow and heat transfer analysis of Williamson nanofluid, *Appl Nanosci.*, DOI 10.1007/s13204-013-0282-1.
- [11] Wang, Y., (1989), Free convection on a vertical stretching surface, *J Appl Math Mech.*, Vol.69, pp.418-420.